ASME 2013 International Design Engineering Technical Conference
& Computers and Information in Engineering Conference
August 04-07, 2013 - Portland, OR, USA

Contact Model between Superelements in Dynamic Multibody Systems

G. VIRLEZ*, O. Brüls, V. Sonneville, E. Tromme, P. Duysinx, M. Géradin

*PhD student – FRIA fellowship

Department of Aerospace and Mechanical Engineering (LTAS)
University of Liège, Belgium

2013-08-07

Contact modeling

Contact between two superelements

- Flexibility accounted for with reasonable CPU time and memory
- Contact forces transferred to load directly the modal variables
  ➔ very compact formulation

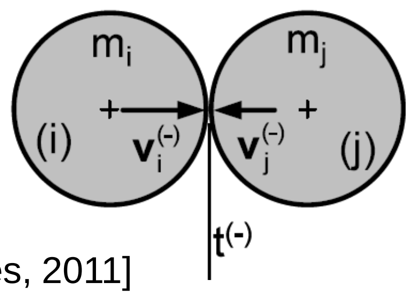

[Flores, 2011]

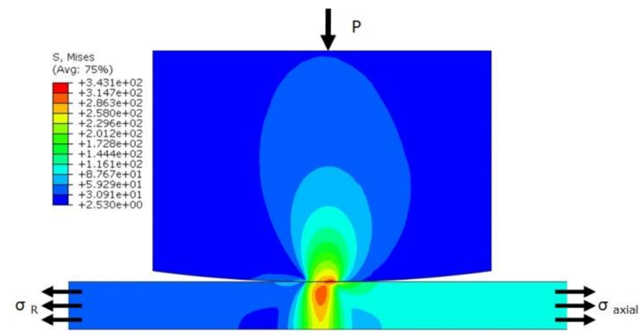

[Hojjati, UGent]

Contact between rigid bodies

⊕ low memory and CPU requirements

⊖ rigidity assumption

Contact between FE models

⊕ Flexibility accurately represented

⊖ CPU time and memory highly expensive

- 2 possible strategies for the contact formulation: penalty versus LCP

Gear pair modeling

- Global model [Cardona, 1995]
  - Kinematic joints defined between 2 nodes (wheel centers).
  - Gear wheels = rigid body.
  - Spring-damper along the normal pressure line.
  - Gross modeling of meshing defaults:
    (backlash, load transmission error, friction,…).

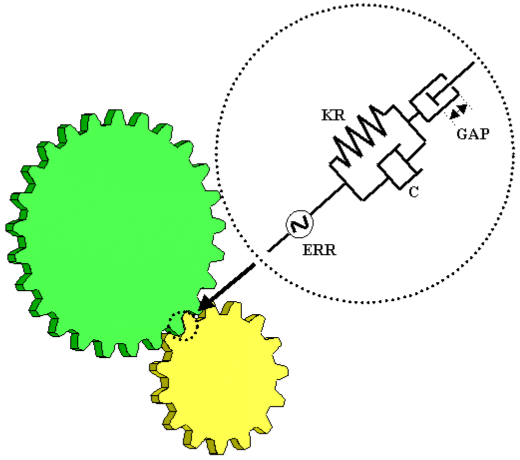

- Contact condition between FE models
  - Deformation of gear teeth and gear web accurately taken into account.
  - Meshing defaults naturally modeled.
  - Short time simulation of 2 gear wheels.

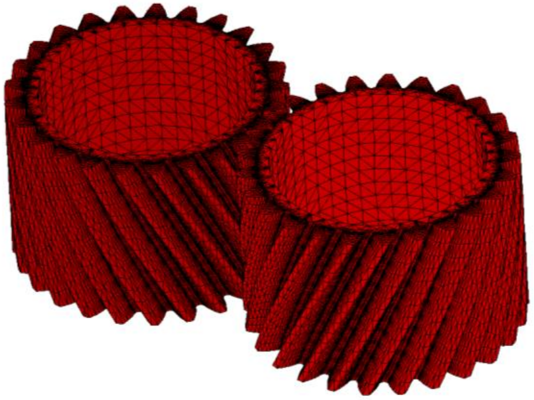

- Contact model between superelements [Ziegler & Eberhard, 2011]
  - Gear wheel flexible behavior globally accounted for.
  - Determination of actual contact points by means of 3D gear wheel geometry.
  - Study of misalignment, backlash, gear hammering,…

Outline

- Corotational formulation of a superelement
- Contact detection algorithm
- Contact force formulation
- Numerical results:
  - Cam system
  - Gear pair simulation
- Ongoing work: dual approach for superelement formulation

Superelement formulation

Craig-Bampton method: substructuring technique for linear elastic model

- Static boundary modes

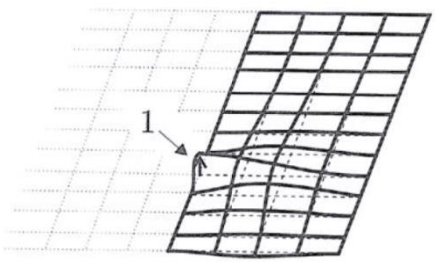

$$\boldsymbol{\Psi}_B = -\boldsymbol{K}_{II}^{-1}\boldsymbol{K}_{IB}$$

- Internal vibration modes

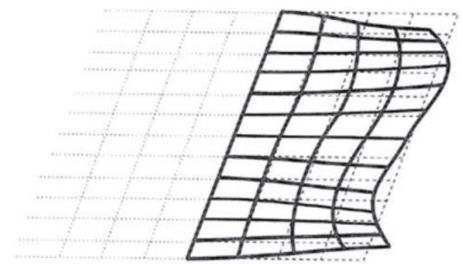

$$\left(\boldsymbol{K}_{II} - \omega^2 \boldsymbol{M}_{II}\right)\boldsymbol{\Psi}_I = \mathbf{0}_{n_I \times n_I}$$

- Reduction basis (mode matrix)

$$\overline{\boldsymbol{\Psi}} = \begin{bmatrix} \boldsymbol{I} & \mathbf{0} \\ \boldsymbol{\Psi}_B & \overline{\boldsymbol{\Psi}}_I \end{bmatrix}$$

- Reduced stiffness and mass matrices

$$\overline{\boldsymbol{K}} = \overline{\boldsymbol{\Psi}}^T \boldsymbol{K} \overline{\boldsymbol{\Psi}} = \begin{bmatrix} \overline{\boldsymbol{K}}_{BB} & \mathbf{0} \\ \mathbf{0} & \boldsymbol{\mu}\,\boldsymbol{\omega}^2 \end{bmatrix} \qquad \overline{\boldsymbol{M}} = \overline{\boldsymbol{\Psi}}^T \boldsymbol{M} \overline{\boldsymbol{\Psi}} = \begin{bmatrix} \overline{\boldsymbol{M}}_{BB} & \overline{\boldsymbol{M}}_{BI} \\ \overline{\boldsymbol{M}}_{IB} & \boldsymbol{\mu} \end{bmatrix}$$

Corotational formulation of a superlement

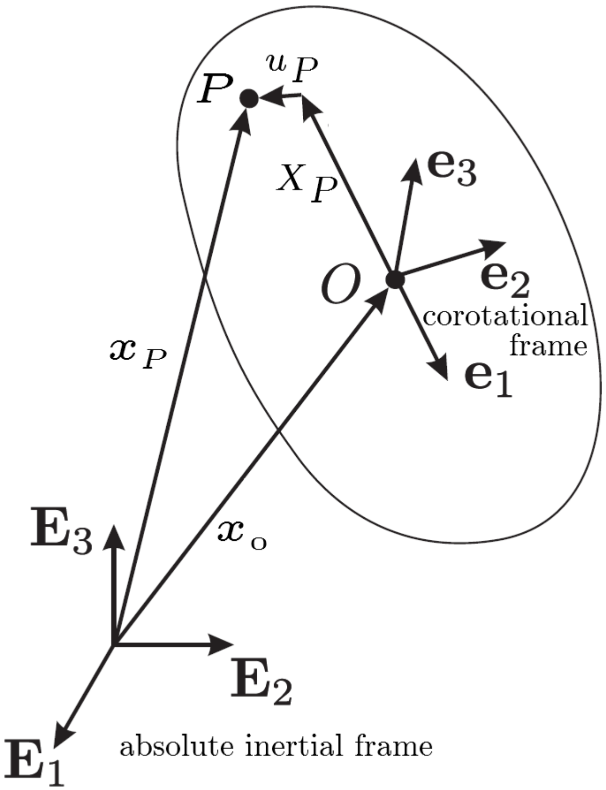

- Kinematics of a superelement

$$\boldsymbol{x}_P = \boldsymbol{x}_0 + \boldsymbol{R}_0(\boldsymbol{X}_P + \boldsymbol{u}_P)$$
$$\boldsymbol{R}_P = \boldsymbol{R}_0 \; \boldsymbol{R}(\gamma_P)$$

- Vector of generalized coordinates

$$\eta = \begin{Bmatrix} \mathbf{u}_B \\ \gamma_B \\ \eta_I \end{Bmatrix} \qquad \mathbf{q} = \begin{Bmatrix} \mathbf{x}_0 \\ \alpha_0 \\ \mathbf{x}_B \\ \alpha_B \\ \eta_I \end{Bmatrix} \qquad \delta\eta = \mathbf{P}(\mathbf{q})\,\delta\mathbf{q}$$

- Elastic forces in the absolute inertial frame

$$\mathbf{g}^{elastic} = \mathbf{P}^T \overline{\mathbf{K}} \eta$$

- Constraints to determine the corotational frame position

$$\Phi(\mathbf{q}) \equiv \tau_{rig}^T \, \overline{\mathbf{M}}_B \, \eta_B(\mathbf{q}) = \mathbf{0}$$

Rigid body modes

$$\tau_{rig} = \begin{bmatrix} \tau_{rig,1} \\ \vdots \\ \tau_{rig,i} \\ \vdots \\ \tau_{rig,nb} \end{bmatrix} \qquad \tau_{rig,i} = \begin{bmatrix} \mathbf{I}_{3\times3} & -\widetilde{\mathbf{X}}_{Bi} \\ \mathbf{0}_{3\times3} & \mathbf{I}_{3\times3} \end{bmatrix}$$

Boundary nodes vs. contact nodes

- If all candidate contact nodes are boundary nodes
  ➔ huge number of generalized coordinates

$$\mathbf{q} = \begin{Bmatrix} \mathbf{x}_0 \\ \alpha_0 \\ \mathbf{x}_B \\ \alpha_B \\ \eta_I \end{Bmatrix}$$

- Solution:
  - A few number of boundary nodes.
  - The position of candidate contact nodes are computed from modal variables and the corotational frame position.

$$\begin{aligned} \boldsymbol{x}_{C_i} &= \boldsymbol{x}_0^s + \boldsymbol{R}_0^s(\boldsymbol{X}_{C_i} + \overline{\boldsymbol{\Psi}}_{C_i}\boldsymbol{\eta}^s) \\ \boldsymbol{x}_{N_i} &= \boldsymbol{x}_0^m + \boldsymbol{R}_0^m(\boldsymbol{X}_{N_i} + \overline{\boldsymbol{\Psi}}_{N_i}\boldsymbol{\eta}^m) \end{aligned}$$

  - Direct loading of the modal variables (static and dynamic).

➔ **very compact formulation**

Contact detection algorithm

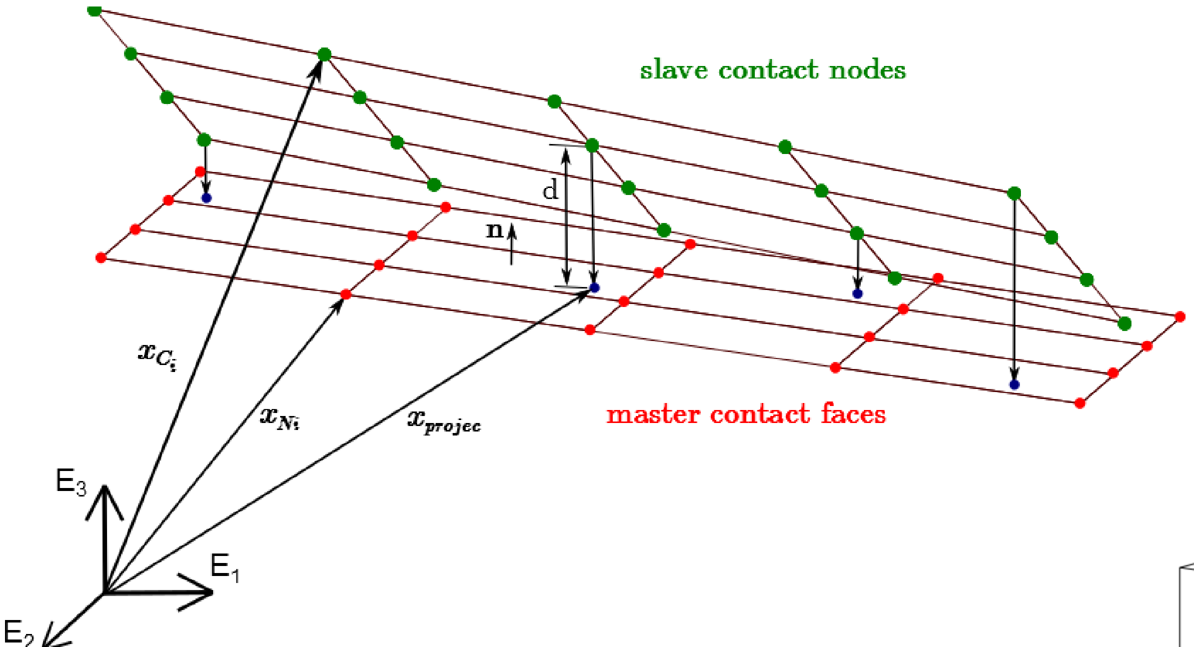

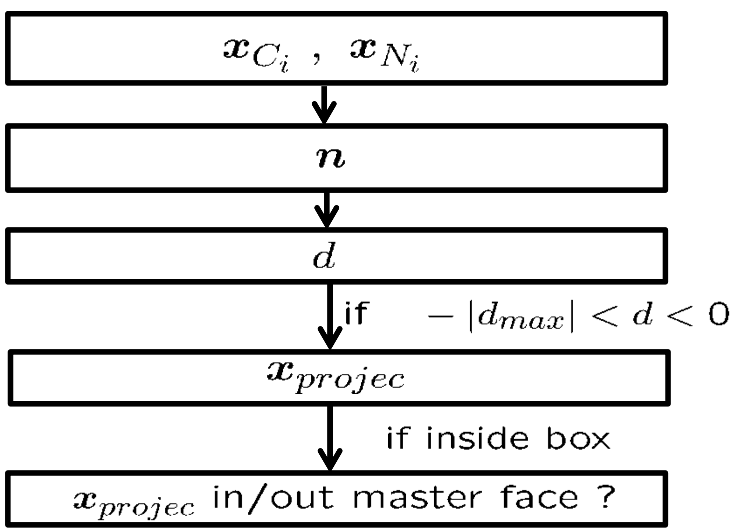

Projection point outside the surface element ➔ inactive contact

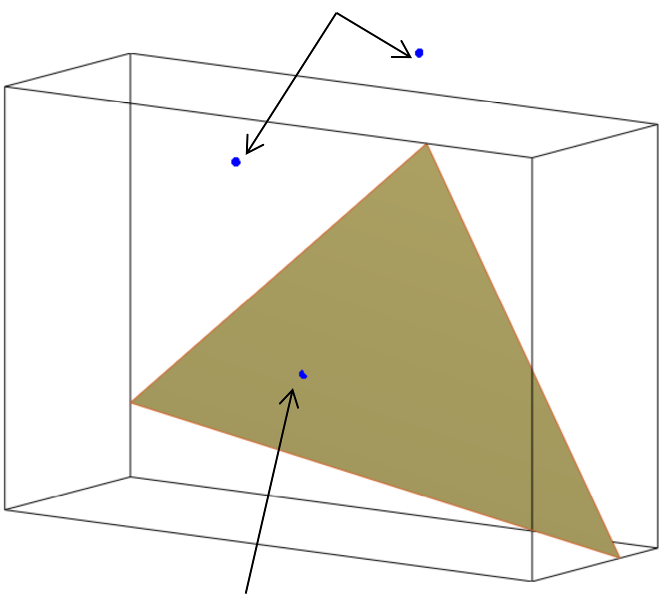

Projection point inside the surface element ➔ active contact

Contact force

- Contact law: penalty method with a stiffness and a damping contribution

$$f(\ell,\dot{\ell}) = \begin{cases} S_c^* \left(k_p\, \ell^n + c\, \ell^n\, \dot{\ell}\right) & \text{if} \quad \ell > 0 \quad \text{active contact} \\ 0 & \text{if} \quad \ell < 0 \quad \text{no contact} \end{cases}$$

penetration length:

$$\begin{aligned} \ell &= \boldsymbol{n}^T(\boldsymbol{x}_{N1} - \boldsymbol{x}_{C_i}) \\ \dot{\ell} &= \boldsymbol{n}^T(\dot{\boldsymbol{x}}_{N1} - \dot{\boldsymbol{x}}_{C_i}) + (\boldsymbol{x}_{N1} - \boldsymbol{x}_{C_i})^T\, \dot{\boldsymbol{n}} \end{aligned}$$

- Contact force vector

$$\boldsymbol{f}_c = \underline{w}\; f\; \boldsymbol{n}$$

participation factor

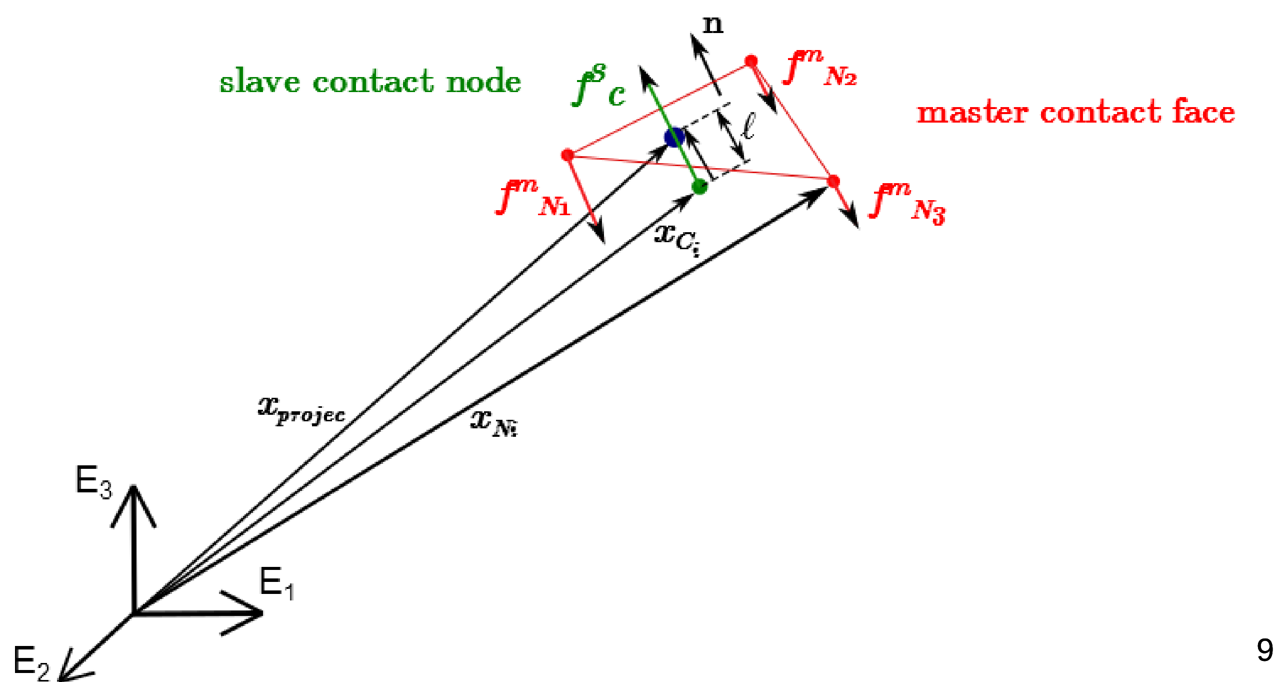

Contact force

- Each force applied on a contact node is transformed in order to load the modal variables of the superelement :

$$\delta W_{C_i}^{con} = \delta \boldsymbol{x}_{C_i}^T \, \boldsymbol{f}_c = \delta \boldsymbol{q}^T \boldsymbol{g}_{C_i}^{int,con}$$

with

$$\delta \boldsymbol{x}_{C_i} = \delta \boldsymbol{x}_0 - \boldsymbol{R}_0 \widetilde{(\boldsymbol{X}_{C_i} + \boldsymbol{u}_{C_i})} \, \delta \boldsymbol{\Theta}_0 + \boldsymbol{R}_0 \, \delta \boldsymbol{u}_{C_i}$$

$(\tilde{\boldsymbol{a}} \; \boldsymbol{b} = \boldsymbol{a} \times \boldsymbol{b})$

$$= \delta \boldsymbol{x}_0 - \boldsymbol{R}_0 \widetilde{(\boldsymbol{X}_{C_i} + \overline{\boldsymbol{\Psi}}_{C_i} \boldsymbol{\eta})} \, \delta \boldsymbol{\Theta}_0 + \boldsymbol{R}_0 \overline{\boldsymbol{\Psi}}_{C_i} \boldsymbol{P} \, \delta \boldsymbol{q}$$

- The internal force vector due to a contact force is expressed as:

$$\boldsymbol{g}_{C_i}^{int,con} = \boldsymbol{P}^T \overline{\boldsymbol{\Psi}}_{C_i}^T \boldsymbol{R}_0^T \, \boldsymbol{f}_c + \begin{Bmatrix} \boldsymbol{f}_c \\ \widetilde{(\boldsymbol{X}_{C_i} + \overline{\boldsymbol{\Psi}}_{C_i} \boldsymbol{\eta})} \boldsymbol{R}_0^T \, \boldsymbol{f}_c \\ \boldsymbol{0} \\ \boldsymbol{0} \\ \boldsymbol{0} \end{Bmatrix}$$

- Analytical computation of its contribution to the iteration matrix

System description

Total number of DOFs: 142

- 18+9 boundary nodes
- 20+20 vibrations nodes

<< 107532 Dofs of full FE model

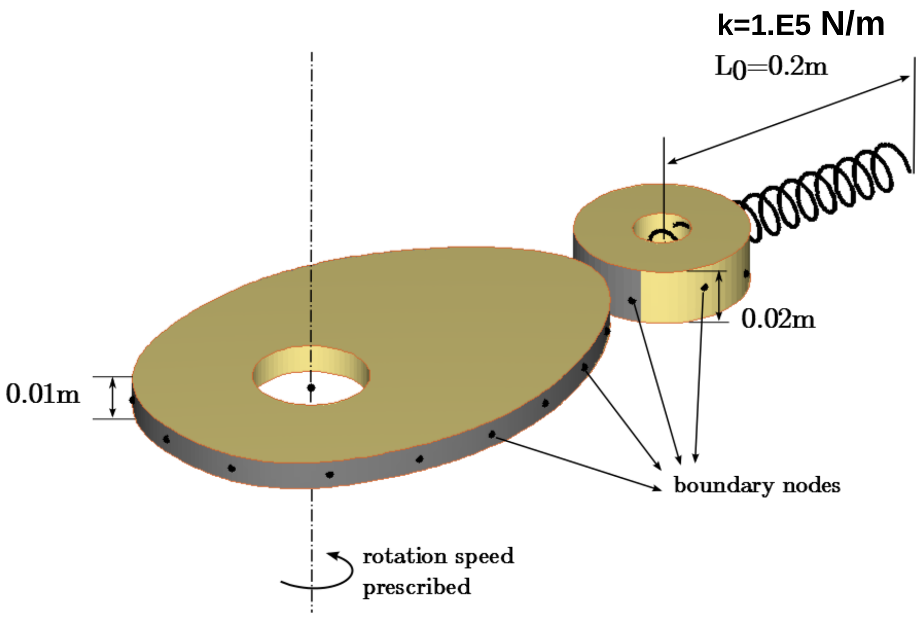

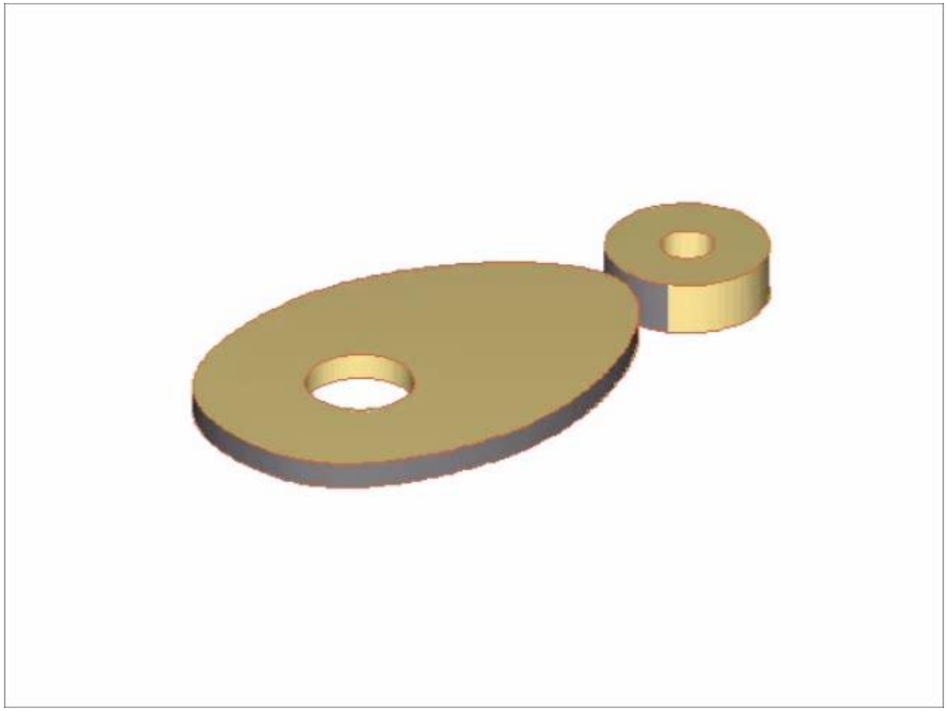

Eigenfrequencies of internal vibration modes (Hz)		
	roller	cam
f_1	2.5E4	4.5E3
f_{20}	6.6E4	2.2E4

Numerical results

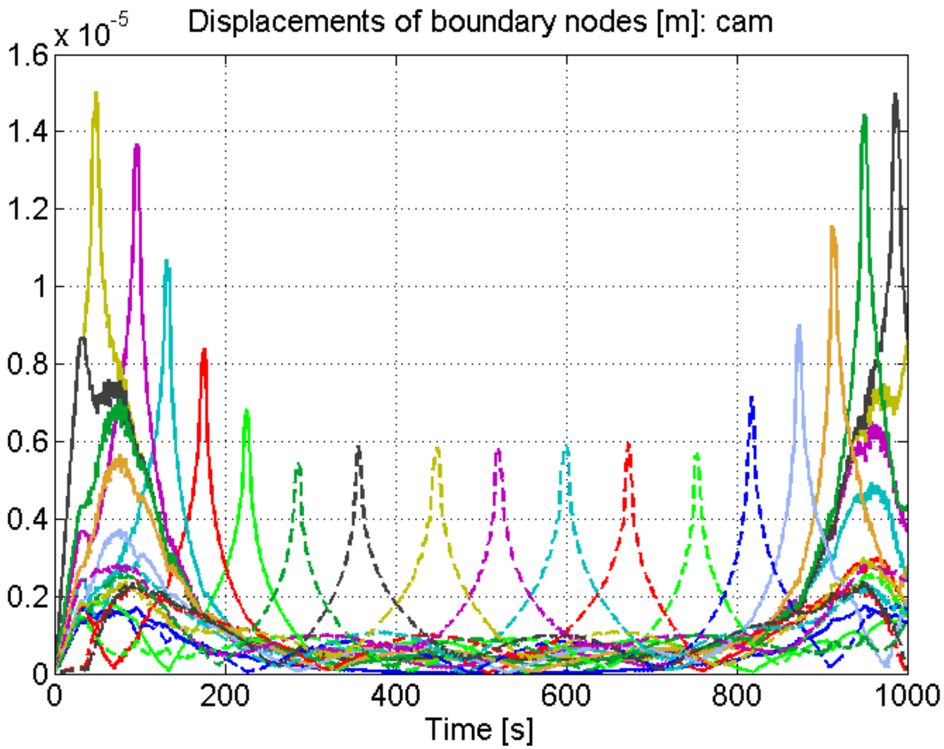

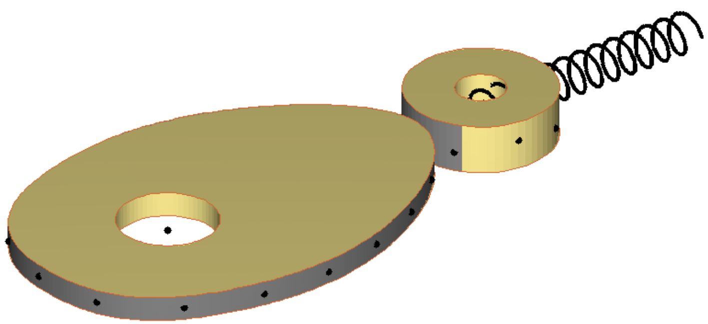

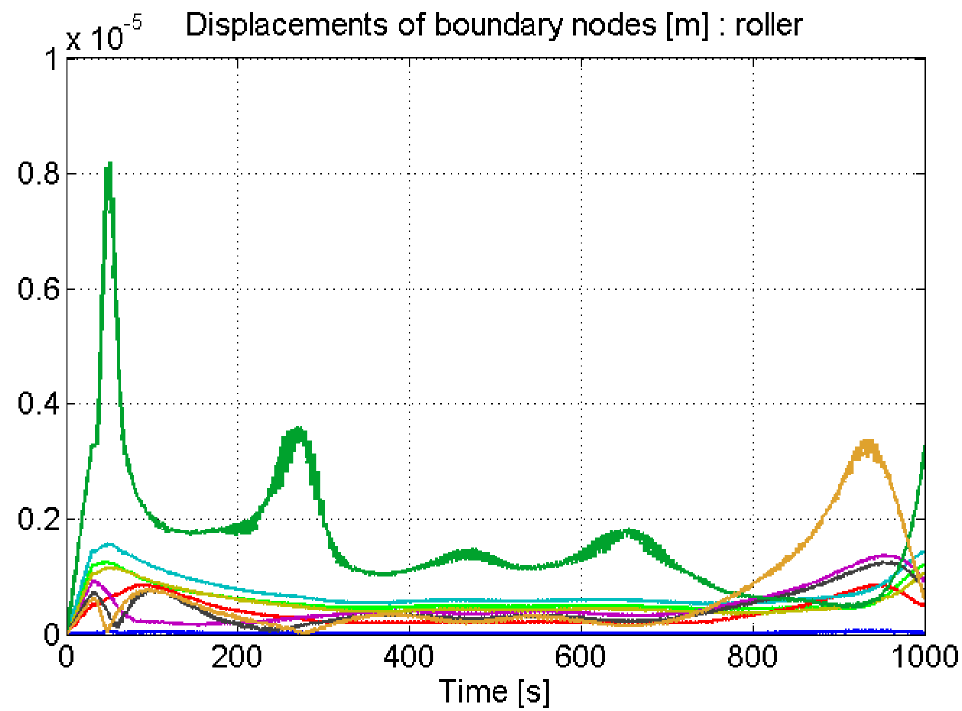

Numerical results

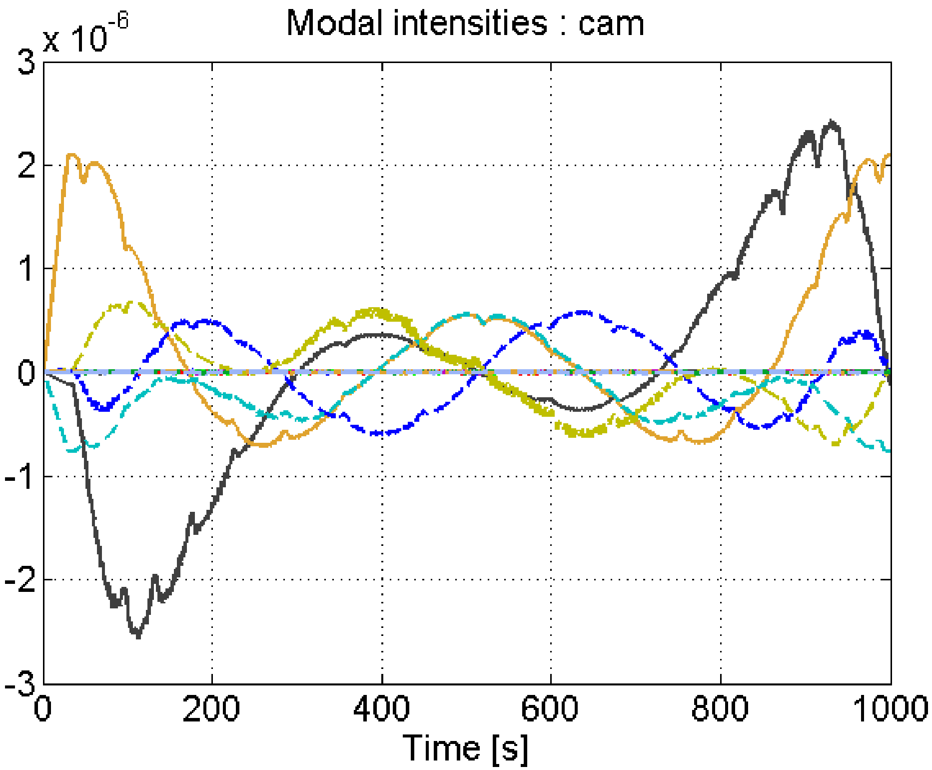

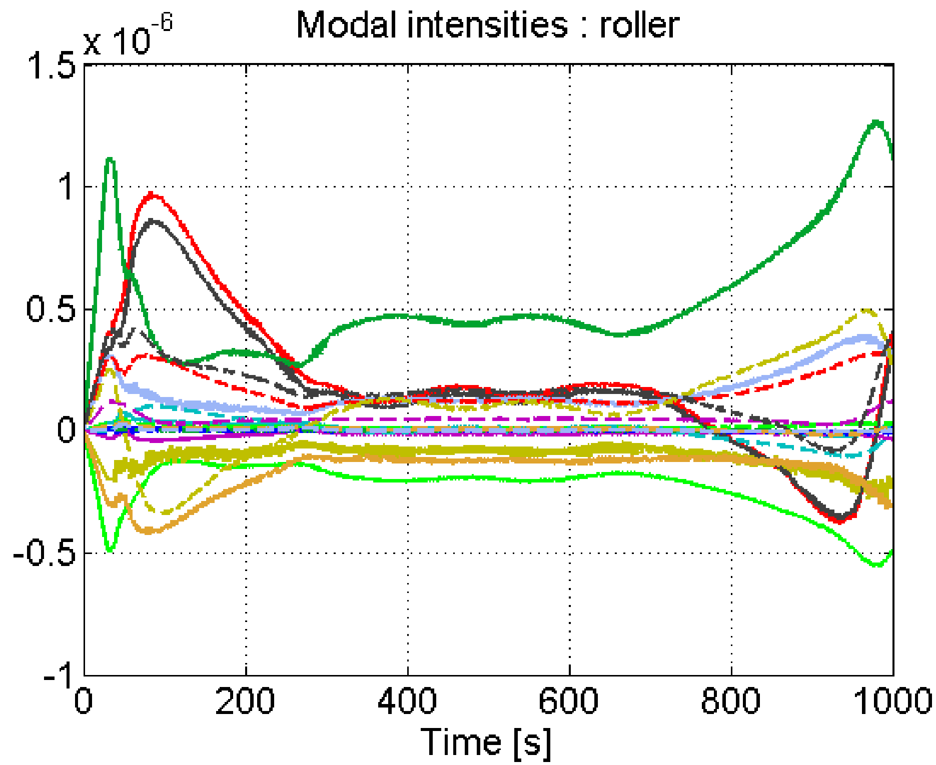

Gear pair modeling: various steps

1) CAD modeling (CATIA V5)

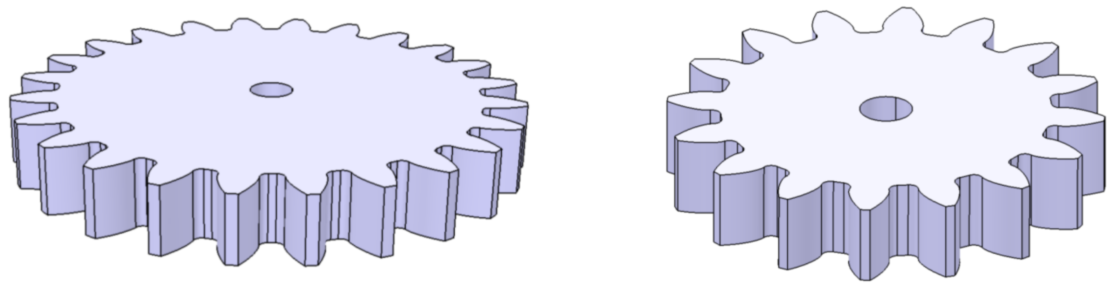

2) FE modeling and model reduction (SAMCEF)

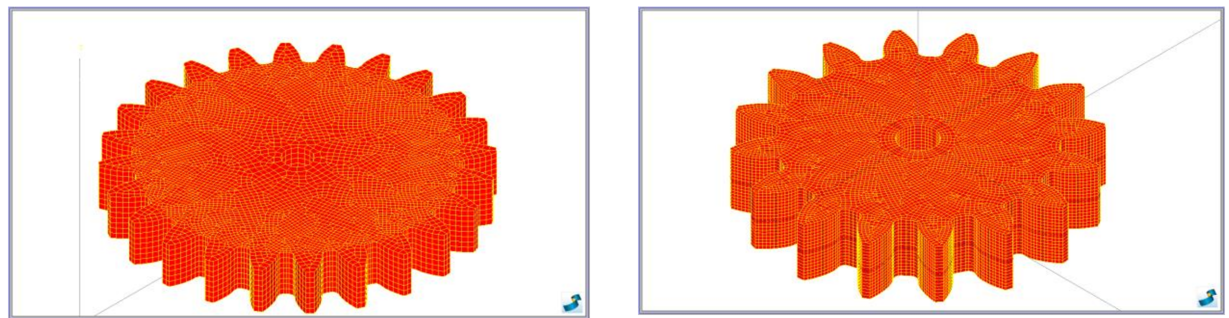

$$\overline{\boldsymbol{K}}, \overline{\boldsymbol{M}}, \overline{\boldsymbol{\Psi}}$$

3) Simulation of unilateral contact between superelements (MATLAB)

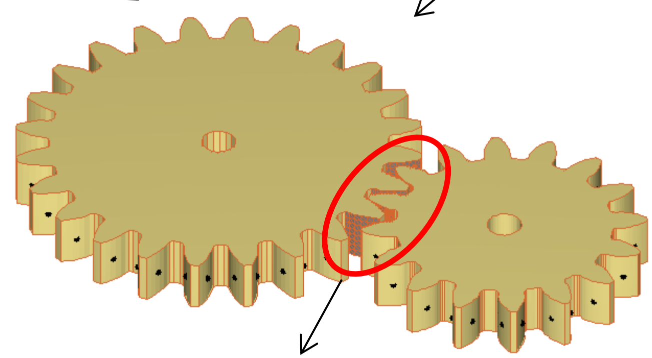

Selection strategy of slave-master flank pairs

Model description

	pinion	gear
Number of teeth [-]	16	24
Pitch diameter [mm]	73,2	109,8
Outside diameter [mm]	82,64	118,64
Root diameter [mm]	62,5	98,37
Addendum coef. [-]	0,196	0,125
Tooth width [mm]	15	
Pressure angle [deg]	20	
Module [mm]	4,5	

(Lundvall, Strömberg, Klarbring, 2004)

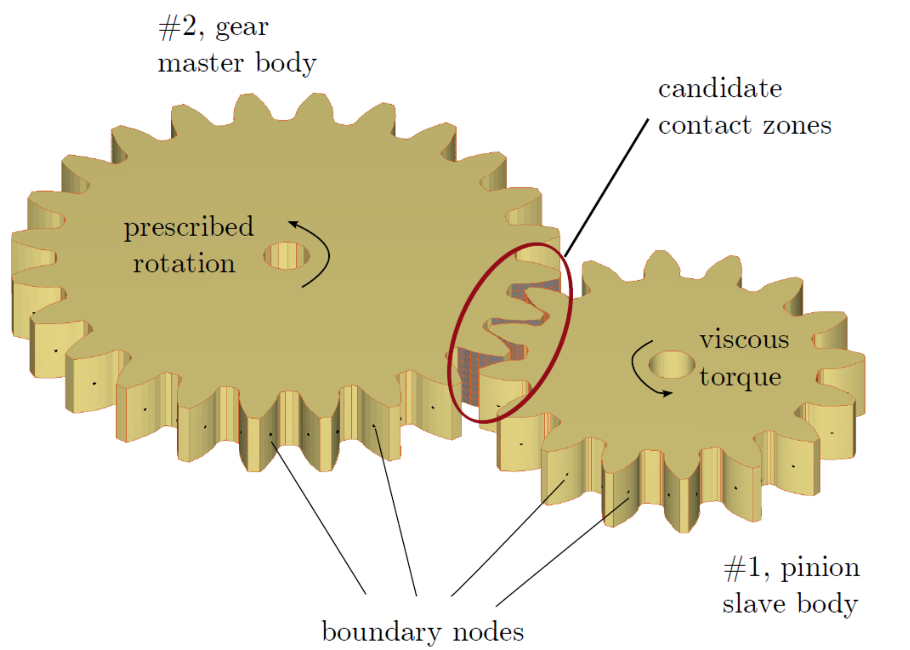

- 1 boundary node per tooth flank
  100 internal vibrations modes
  ➔ 695 DOFS << 480171 for FEM
- Parallel rotation axis ➔ no misalignment
- Large center distance ➔ significant backlash
- At t=0s, ω_1 = -1000 rpm , ω_2= 667 rpm
- For t > 0s : Viscous torque: $T_1 = -1\ \omega_1$; ω_2= 667 rpm
- Time step: h=1E.-6s

Eigenfrequencies of internal vibration modes (Hz)		
	pinion	gear
f_1	19520	10402
f_{100}	146068	115469

Numerical results

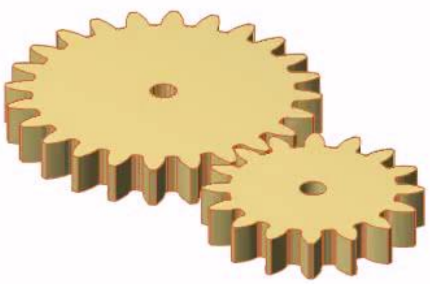

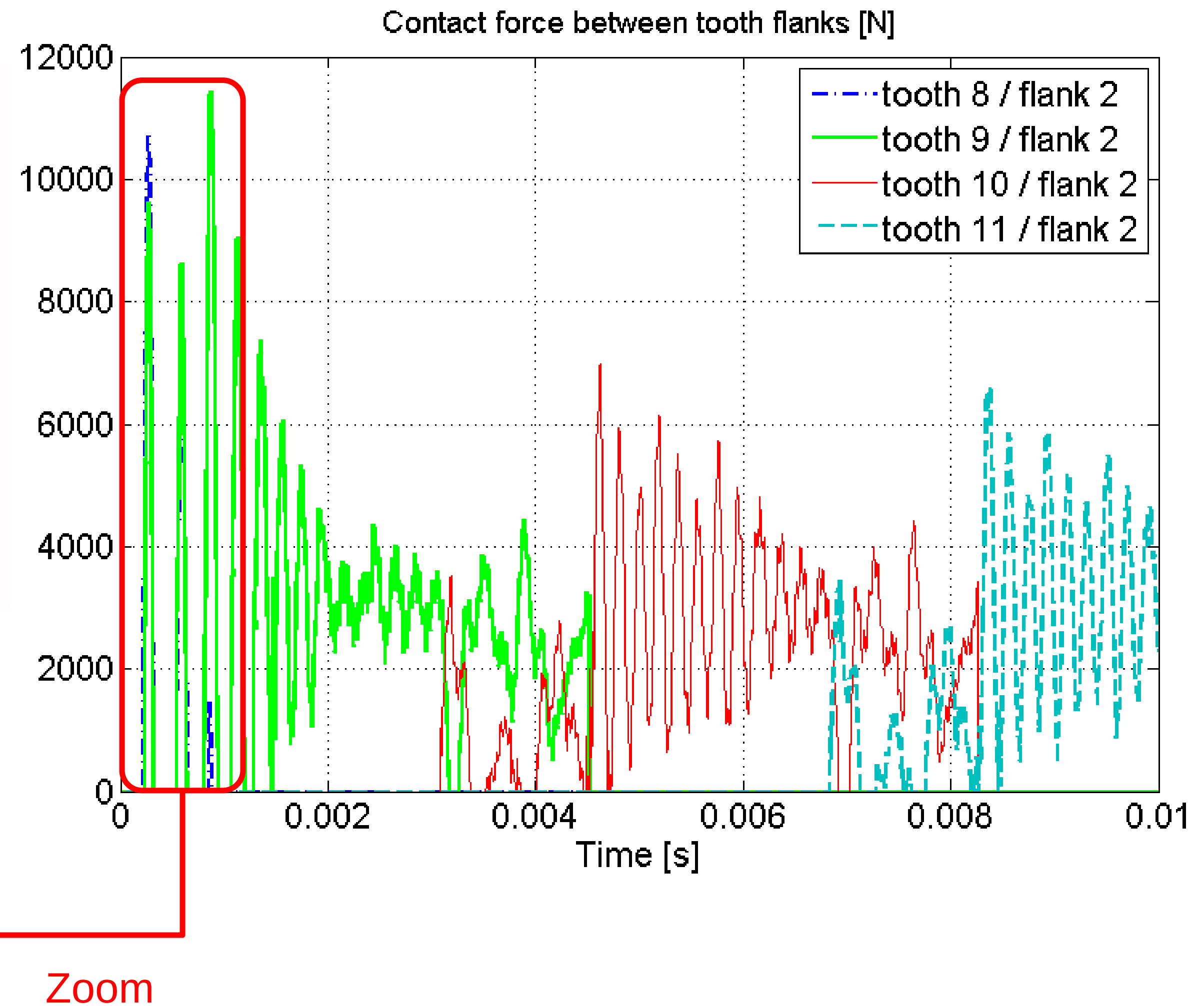

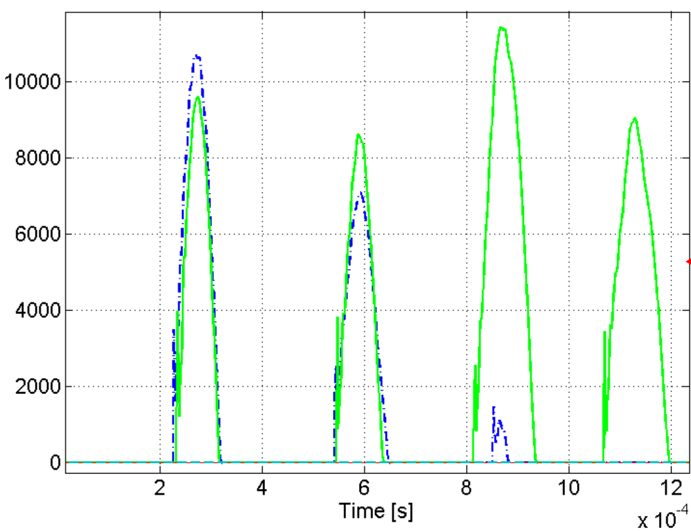

Numerical results

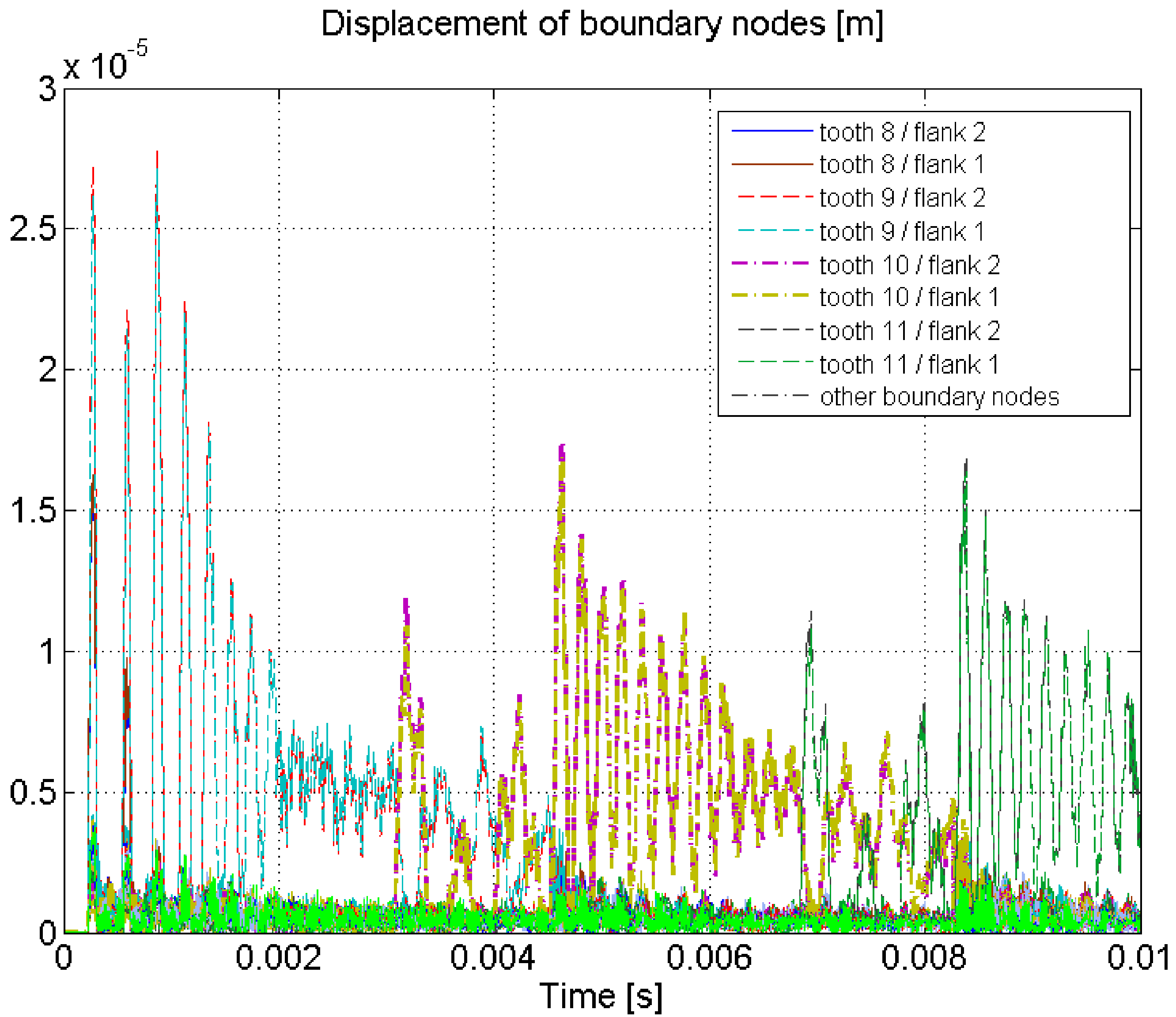

Numerical results

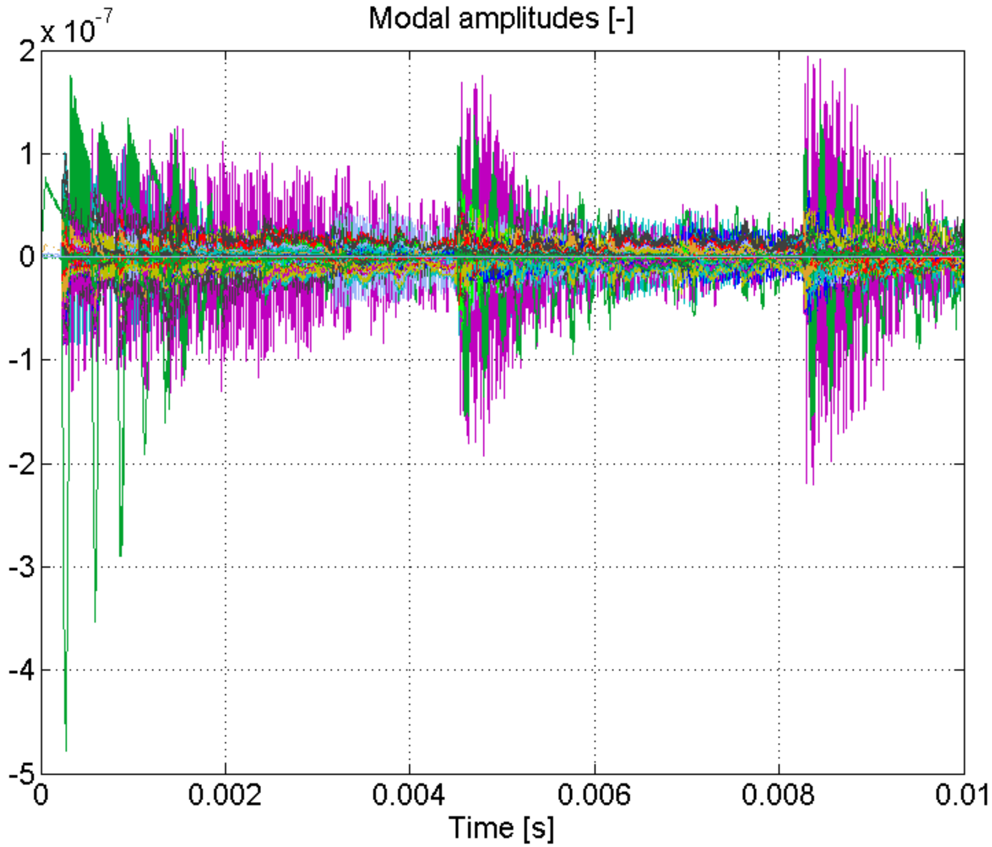

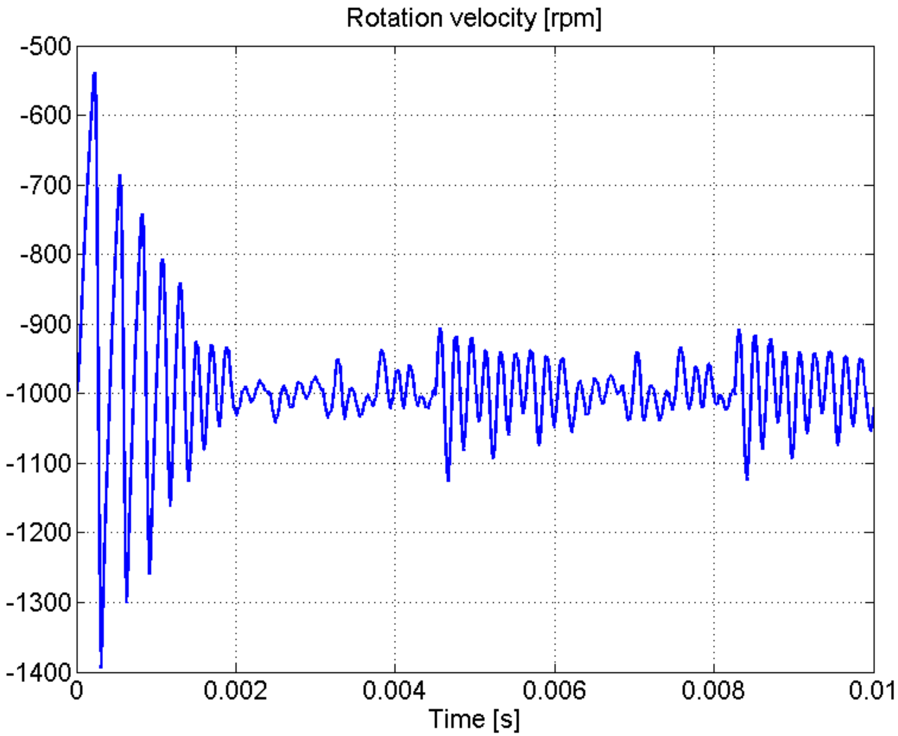

Ongoing work: dual approach

- Dual Craig-Bampton [Rixen, 2004]
  - Subset of free-free vibration modes

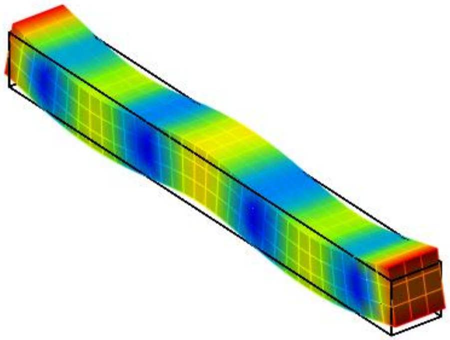

  - Attachment modes to have a correct static response at interface nodes

    ~~Unit displacements~~ ➔ unit loads

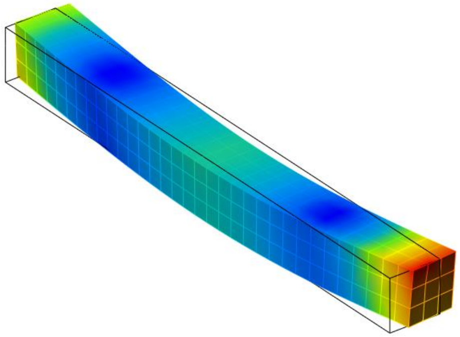

Filtering with respect to the elastic modes
➔ **residual** attachment modes

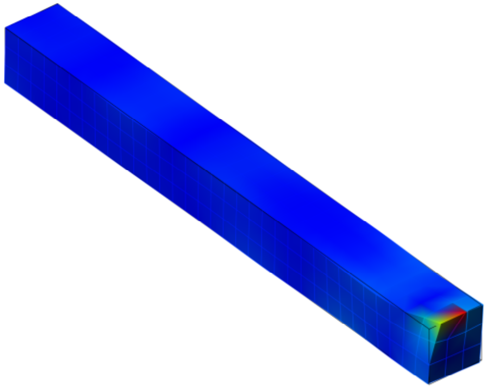

- Mode matrix

$$\overline{\mathbf{\Psi}} = \begin{bmatrix} \overline{\mathbf{\Psi}}_f & \mathbf{\Psi}_r \end{bmatrix}$$

Ongoing work: dual approach

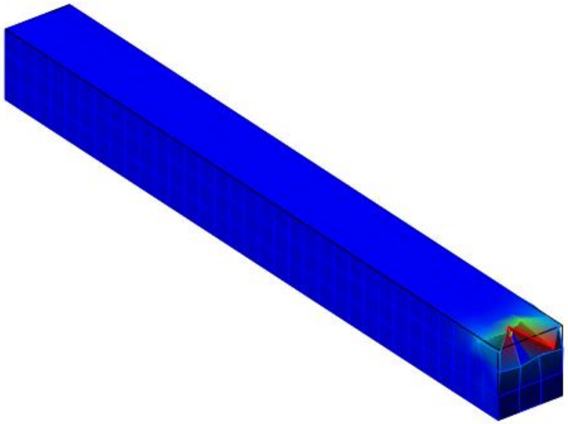

- Residual attachment modes can be orthogonalized in order to get full diagonal matrices

$$\overline{\boldsymbol{K}} = \begin{bmatrix} \omega_f^2\, \boldsymbol{\mu}_f & \mathbf{0} \\ \mathbf{0} & \omega_r^2\, \boldsymbol{\mu}_r \end{bmatrix} \qquad \overline{\boldsymbol{M}} = \begin{bmatrix} \boldsymbol{\mu}_f & \mathbf{0} \\ \mathbf{0} & \boldsymbol{\mu}_r \end{bmatrix}$$

- Floating frame to describe the rigid body motion of the superlement instead of corotational frame

$$\boldsymbol{q} = \begin{Bmatrix} \boldsymbol{x}_0 \\ \boldsymbol{\alpha}_0 \\ \boldsymbol{\eta}_f \\ \boldsymbol{r} \end{Bmatrix} \qquad \boldsymbol{u} \cong \overline{\boldsymbol{\Psi}}_f\, \boldsymbol{\eta}_f + \boldsymbol{\Psi}_r\, \boldsymbol{r}$$

- Main difference with respect to MacNeal and Rubin methods:

  ➔ assembly with interface forces rather than interface displacements

- Contact element unchanged

$$\begin{Bmatrix} \boldsymbol{x}_0 \\ \boldsymbol{\alpha}_0 \\ \boldsymbol{\eta} \end{Bmatrix} \longrightarrow \boldsymbol{x}_{C_i} \longrightarrow \text{Contact detection algorithm} \longrightarrow \boldsymbol{f}_c \longrightarrow \begin{Bmatrix} \boldsymbol{f}_c \\ \widetilde{(\boldsymbol{X}_{C_i} + \overline{\boldsymbol{\Psi}}_{C_i}\boldsymbol{\eta})}\, \boldsymbol{R}_0^T\, \boldsymbol{f}_c \\ \overline{\boldsymbol{\Psi}}_{C_i}^T \boldsymbol{R}_0^T\, \boldsymbol{f}_c \end{Bmatrix}$$

SE generalized coordinates | Position of candidate contact nodes | Contact force | Loading of SE coordinates

Conclusion

- Summary
  - Reduction of model size by 1 to several orders of magnitude
  - Direct loading of the modal generalized variables
- Perspectives:
  - Improvement of the contact detection algorithm
  - Dynamic management of contact zones (mode switching)
  - Contact law with algebraic constraint and nonsmooth time integration
  - Friction forces
  - Testing in various configurations (e.g. misalignment,…)
  - Implementation in a commercial software
  - Simulation of a full TORSEN differential

Thank you for your attention !

Contact Model between Superelements in Dynamic Multibody Systems

Geoffrey VIRLEZ

Email: geoffrey.virlez@ulg.ac.be

- Acknowledgements:
  - The Belgian National Fund for Scientific research (FNRS-FRIA)
  - The industrial partners: LMS-SAMTECH
    JTEKT TORSEN EUROPE